

Wigner crystals of Na⁺ ions at the surface of a silica hydrosol

Aleksey M. Tikhonov^{a)}

Consortium for Advanced Radiation Sources, University of Chicago, Argonne, Illinois 60439
and Brookhaven National Laboratory, National Synchrotron Light Source, Beamline X19C,
Upton, New York 11973

(Received 16 January 2007; accepted 29 March 2007; published online 4 May 2007)

The symmetry of the surface of an electrolyte solution can be anisotropic, regardless of the bulk's isotropic symmetry, because of spatial correlations between adsorbed ions. The author used x-ray grazing-incidence diffraction to measure the spatial correlations between sodium ions in "classical one-component plasma" adsorbed with Bjerrum's density at the surface of a monodispersed 22 nm particle colloidal silica solution stabilized by NaOH with a total bulk concentration ~ 0.05 mol/L. The authors findings show that the surface compact layer is in a two-dimensional crystalline state (symmetry $p2$), with four sodium ions forming the unit cell and a ~ 30 Å translational correlation length between the ions. © 2007 American Institute of Physics. [DOI: 10.1063/1.2734542]

With a density of adsorbed ions as high as Bjerrum's density at a liquid's surface, the average energy of their electrostatic interactions is comparable to their thermal energy, so that the ions can transit into a two-dimensional condensed phase.¹ Earlier, several authors proposed that ions adsorbed at a strongly charged macroion in a colloidal solution form a two-dimensional strongly correlated liquid in which the short order of ions is similar to that of a Wigner crystal.²⁻⁷ In this paper, I discuss my x-ray grazing-incidence diffraction study of the spatial correlations between sodium ions adsorbed at the free surface of a monodisperse colloidal silica solution, wherein the average distance between them, $\xi \sim 5$ Å, is less than the Bjerrum radius for monovalent ions in aqueous media, ~ 7 Å. According to my data, the surface compact layer is in a two-dimensional crystalline state with a translational correlation length of ~ 30 Å between the sodium ions. As far as I am aware, this is the first report on the crystallization of two-dimensional ions in "classical one-component plasma" adsorbed with Bjerrum's density at the free surface of a liquid. Previously, a number of studies have probed the planar surfaces of aqueous electrolyte solutions with various surface-sensitive x-ray scattering techniques.⁸⁻¹³ In some cases, authors suggested that in-plane correlations were possible between adsorbed ions because of the specific interactions of the electrolyte ions with either a surface of a solid crystal or of a crystalline lipid monolayer (membrane).

My recent x-ray scattering studies of the surface of the nanocolloidal silica solutions stabilized by NaOH ($pH \sim 9-10$) revealed a spontaneously formed nontrivial surface-normal structure that reflects a colossal difference in the potentials of "image forces" for cationic alkali ions and anionic nanoparticles [Fig. 1(a)].^{14,15} At room temperature, the structure consists of a 2-nm-thick compact layer of Na⁺ with a surface concentration $\Gamma^+ \sim 10^{19}$ m⁻² and an underlying loose monolayer of nanocolloidal particles as part of a thick diffuse layer, in between which is a layer with a low concen-

tration of electrolytes (water layer).¹⁶ According to my previous x-ray reflectivity study, the compact layer can be described by a two-layered model, i.e., a ~ 6 -Å-thick low-density layer (layer 1) of directly adsorbed hydrated alkali ions with a surface concentration $\Gamma_1^+ \sim 3 \times 10^{18}$ m⁻² and a ~ 13 -Å-thick high-density layer (layer 2) with a surface concentration of sodium ions $\Gamma_2^+ \sim 8 \times 10^{18}$ m⁻².¹⁴ The main difference between them is their alkali ion/water ratio: the number of H₂O molecules per ion in the low-density layer 1 with a total surface density of electrons in it, $\Gamma_1 \sim 10^{20}$ m⁻², is as much as $(\Gamma/10 - \Gamma_1^+)/\Gamma_1^+ \sim 2$ (both Na⁺ and H₂O contain ten electrons); however, the number of H₂O molecules per Na⁺ in layer 2 is much larger, $(\Gamma/10 - \Gamma_2^+)/\Gamma_2^+ \sim 10$, where $\Gamma_2 \sim 7 \times 10^{20}$ m⁻² is the total surface density of electrons in this layer. Therefore, the dielectric permittivity ϵ in layer 1 must be approximately five times less than that in layer 2, so that the interaction between ions in layer 1 is stronger ($R_B \sim 1/\epsilon$) than in layer 2, since $\xi \approx (l_1/\Gamma_1^+)^{1/3} \approx (l_2/\Gamma_2^+)^{1/3} \sim 5-6$ Å is roughly the same for both layers.

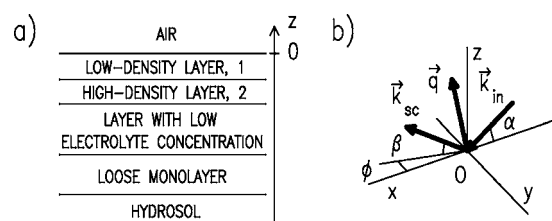


FIG. 1. (a) The surface-normal structure of the silica hydrosol's surface. It consists of a 2-nm-thick compact layer of Na⁺ with the surface concentration Γ^+ as large as $\sim 10^{19}$ m⁻², a loose monolayer of nanocolloidal particles (~ 20 nm thick) as part of a thick diffuse layer, in between which is a ~ 15 -nm-thick layer with low electrolyte concentration. The compact layer can be described by a two-layer model, i.e., a ~ 6 -Å-thick low-density layer (layer 1) of directly adsorbed hydrated alkali ions and a ~ 13 -Å-thick high-density layer (layer 2) (Ref. 4). (b) Sketch of the kinematics of the scattering at the silica sol's surface. The xy plane coincides with the interface, the y axis is perpendicular to the beam's direction, and the z axis is directed normal to the surface opposite to the gravitational force. \mathbf{k}_{in} and \mathbf{k}_{sc} are, respectively, wave vectors of the incident beam and beam scattered toward the point of observation, and $\mathbf{q} = \mathbf{k}_{in} - \mathbf{k}_{sc}$.

^{a)}Electronic mail: tikhonov@bnl.gov

I explored the surface of a silica sol containing 22 nm particles to help interpret the diffraction data. Advantageously, the penetration length Λ (~ 10 nm) of the x rays in the grazing-incidence diffraction experiment at the sol's surface was noticeably smaller than the width of the surface transitional region: the plane of the closest approach of the nanoparticles to the surface lies ~ 15 nm beneath it, such that a thick layer of water well separates the compact layer from the silica particles. The particles are repelled from the hydrosol's surface by the electrical imaging force, and hence, their surface concentration is very small.^{14,16}

X-ray grazing-incidence diffraction is the standard technique for looking at the in-plane structure at solid and liquid surfaces with atomic spatial resolution.¹⁷⁻¹⁹ I studied the in-plane structure of eight liquid samples using a synchrotron x-ray liquid surface spectrometer at beamline X19C, National Synchrotron Light Source, Brookhaven National Laboratory,²⁰ employing a monochromatic focused x-ray beam ($\lambda=0.825\pm 0.002$ Å) to explore the hydrosol's planar surface. Samples of colloidal silica (Ludox TM 40, supplied by Grace Davison²¹) in a ~ 100 ml capacity glass dish with a circular interfacial area (100 mm diameter) were equilibrated at $T=298$ K inside a vapor-tight single-stage thermostat and mounted above the level of water in the bath (~ 200 mm diameter), which served as a humidifier. The surface tension of the sol's surface was as large as 74 mN/m, as measured by the Wilhelmy plate method.

The kinematics of scattering at the liquid's surface can be advantageously described within a right-handed rectangular coordinate system wherein the origin O is in the center of the x-ray footprint; here, the xy plane coincides with the air/sol interface, the y axis is perpendicular to the beam's direction, and the z axis is directed normal to the interface opposite to the gravitational force. In the insert in Fig. 1(b), α is the incident angle in the xz plane, β is the angle in the vertical plane between the scattering direction and the interface, and ϕ is the angle in the xy plane between the incident beam's direction and the direction of scattering. At incident angles below critical, $\alpha_c \approx 0.09^\circ$, a monochromatic 15 keV x-ray beam is totally reflected from the sol's surface.¹⁴ At $\alpha < 0.8\alpha_c$, the penetration depth Λ of the x rays is very shallow and scattering occurs in the top $\sim \lambda/(2\pi\alpha_c) \sim 100$ Å thick layer, where the intensity is usually expressed as a function of the in-plane component of the wave-vector transfer $q_{xy} = (q_x^2 + q_y^2)^{1/2}$.¹⁹ At $\alpha, \beta \ll 1$, $q_{xy} \approx (4\pi/\lambda)\sin(\phi/2)$.

Figure 2 depicts the intensity of scattering from the surface of the hydrosol that contains three diffraction peaks. It was recorded at a grazing angle $\alpha \approx 0.07^\circ$ with a vertical position-sensitive detector (Ordela) by summing ten channels covering the range of $\Delta\beta \sim 0.1^\circ$ ($\Delta q_z \sim 2 \times 10^{-2}$ Å⁻¹) at $q_z \approx 0.08$ Å⁻¹. In this experiment, the incident beam's vertical size, set by input slits, was as large as ~ 40 μm, and the horizontal resolution of the detector, set by Soller slits, was as high as $\Delta q_{xy} \approx 0.02$ Å⁻¹ ($\Delta\phi \approx 0.18^\circ$). Figure 3 illustrates the distribution of intensity of grazing-incidence scattering in the q_z vs q_{xy} plane, where the diffraction peaks were recorded by summing ~ 400 channels divided into ~ 30 groups (the number of horizontal lines in the image).

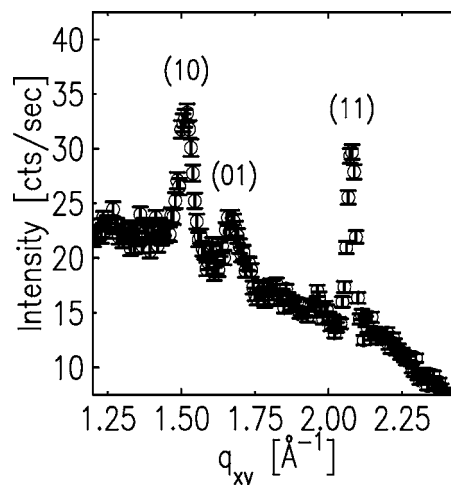


FIG. 2. The intensity of grazing-incidence diffraction at ambient conditions from the surface of the aqueous solution of a suspension of 22 nm silica particles. It was recorded at a glancing angle $\alpha \approx 0.07^\circ$ with a vertical position-sensitive detector (Ordela) by summing ten channels over a range of $\Delta\beta \sim 0.1^\circ$ ($\Delta q_z \approx 0.02$ Å⁻¹) at $q_z \approx 0.08$ Å⁻¹. The detector's horizontal resolution, set by the Soller slits, was as much as $\Delta q_{xy} \approx 0.02$ Å⁻¹ ($\Delta\phi \approx 0.18^\circ$).

The diffraction pattern in Fig. 3 can be qualitatively explained based on the surface-normal model shown in Fig. 1(a). The structure factor of such an "interfacial sandwich" is a set of "Bragg rods" normal to the surface plane at $q_z^2 \ll q_{xy}^2$.¹⁷⁻¹⁹ Fortunately, bulk water and the water's surface scatter x rays very similarly. For example, the grazing-incidence scattering from the surface of water at $q_z=0$ and the intensity of scattering from bulk water have a broad diffraction peak at ~ 2 Å⁻¹ associated mainly with the O-O correlations in water at distances ~ 3 Å.^{14,22} The diffraction peaks in Fig. 2 correspond to the in-plane correlations at noticeably larger distances (~ 4 Å) and cannot be related to scattering in the water layer. On the other hand, the average distance between ions in layers 1 and 2 is $\xi \sim 5-6$ Å, so that the narrow diffraction peaks could reflect two-dimensional crystallization of the hydrated Na⁺ in them.

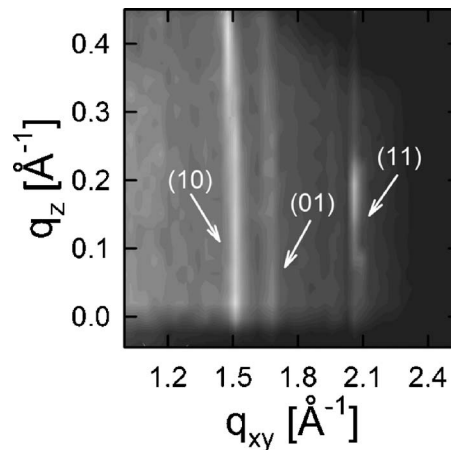


FIG. 3. The intensity of grazing-incidence scattering in the q_z vs q_{xy} plane. It was recorded at a grazing angle of $\alpha \approx 0.07^\circ$ summing ~ 400 channels of the position-sensitive detector divided into ~ 30 groups (number of horizontal lines in the image).

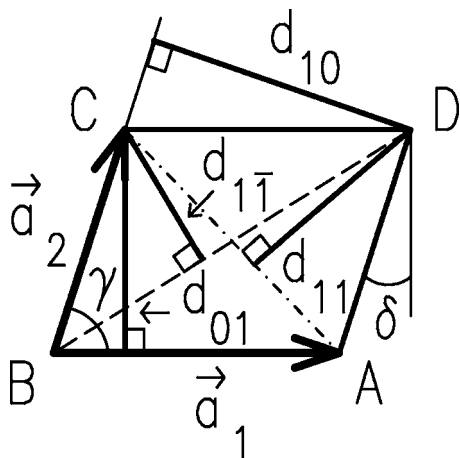


FIG. 4. The oblique unit cell of the two-dimensional Bravais lattice of Na⁺ (symmetry $p2$) at the hydrosol's surface: $a_1 \approx 3.7$ Å, $a_2 \approx 4.1$ Å, and $\gamma \approx 80^\circ$. Sodium ions are centered at the corners of the parallelogram $ABCD$: the dashed line (AC) is the $(1\bar{1})$ row and dash-dotted (BD) line is (11) row. A small deviation of γ from $\pi/2$, δ , can be established, for example, from the equation for the area of the parallelogram $ABCD$, $ACd_{11} = a_2d_{10}$.

The diffraction pattern can be described by an oblique two-dimensional Bravais lattice (symmetry $p2$) defined by two planar vectors a_1 and a_2 of the lattice translations and an angle γ between them, with four Na⁺ forming a unit cell (Fig. 4).²³ Since the distance between the first two peaks at $q_{xy}^{10} \approx 1.5$ Å⁻¹ and $q_{xy}^{01} \approx 1.7$ Å⁻¹ is relatively small, the lattice deviates slightly from the square net ($a_1 = a_2 = a$, $\gamma = \pi/2$). If the splitting of the (10) -reflection, $\kappa = a(q_{xy}^{01} - q_{xy}^{10})/4\pi \approx 0.05$, for the square lattice with period $a = 4\pi/(q_{xy}^{10} + q_{xy}^{01}) \approx 3.9$ Å, then, in accordance with the Bragg-Wulff law, the first two rods immediately denote the distances between ionic rows with the lowest indices in the lattice $d_{10} \approx a(1 + \kappa) \approx 4.1$ Å and $d_{01} \approx a(1 - \kappa) \approx 3.7$ Å. The position of the third peak at $q_{xy}^{11} \approx 2.07$ Å⁻¹ ($d_{11} = 2\pi/q_{xy}^{11} \approx 3.0$ Å) differs from the position of the (11) -reflection for the square lattice ($= 2\sqrt{2}\pi/a \approx 2.3$ Å⁻¹). It can be related to a small deviation of γ from $\pi/2$ that is established from the equation for the area of the parallelogram $ABCD$, $ACd_{11} = a_2d_{10}$ (see Fig. 4). If $\delta = \pi/2 - \gamma \ll 1$, then $AC \approx \sqrt{2}a(1 - \delta/2)$. Since $a_2d_{01} \approx a^2$, then $\delta \approx 2 - \sqrt{2}(a/d_{11}) \approx 0.2$, so that $a_1 \approx d_{10} \approx 4.1$ Å, $a_2 \approx d_{01} \approx 3.7$ Å, and $\gamma \approx 80^\circ$. However, the $(1\bar{1})$ -reflection at $q_{xy}^{1\bar{1}} \sim 2.5$ Å⁻¹ [$d_{1\bar{1}} \approx a(1 - \delta/2)/\sqrt{2} \approx 2.5$ Å] was not observed, possibly due to lattice fluctuations that usually suppress the intensities of diffraction peaks at large q 's.^{23,24}

In Fig. 2 all diffraction peaks have roughly the same width, $\Delta Q_{xy} \sim 0.05$ Å⁻¹ along q_{xy} , which is noticeably larger than the in-plane resolution of the experiments, i.e., Δ_{xy} . Their width signifies that the translational correlation length L between sodium ions in the crystal is as large as $L \sim a^2/\Delta a \sim \pi(a/\Delta Q)^{1/2} \approx 30$ Å, where $\Delta Q = (\Delta Q_{xy}^2 - \Delta_{xy}^2)^{1/2}$ and $\Delta a \sim a^{3/2}\Delta Q^{1/2}/\pi \sim 0.5$ Å is the average deviation of an ion from its site in the lattice.²⁴ I suggest that long-range order is destroyed by spatial fluctuations in the interfacial electric field due to the finite size of the silica nanoparticles, so the diffraction pattern seen in Figs. 2 and 3 is averaged over all crystallites inside the beam's footprint (so-called powder averaging). I also note that Δa explains the large

range of Δq_{xy} where, for example, the (10) -reflection is observed: Laue's diffraction conditions for q are fulfilled within the range, $\Delta q_{xy} \approx 2\pi\Delta a/a^2 \sim 0.2$ Å⁻¹.

The area of the unit cell in an oblique model lattice is as large as $d_{10}d_{01} \approx 15$ Å², i.e., it can accommodate one water molecule. Reasonably, I suggest that the projection of the oxygen atom of the water molecule in the unit cell is centered at the intersection of the diagonals AC and BD in Fig. 4: water molecules form the same oblique lattice as does Na⁺. Possibly, the intensity of (11) -reflection is not constant along q_z because of the tilt of the water molecules in the lattice.¹⁹ Although the symmetry of the lattice $p2$ reflects the anisotropy of the water molecules (point group $mm2$), their exact orientation in the crystal was not established; obtaining this data requires a quantitative analysis of the diffraction data.

The surface density of ions in the crystal, $\Gamma_0^+ \approx 6 \times 10^{18}$ m⁻², is twice as large as Γ_1^+ (the layer with the strongest ion-ion in-plane interaction), as established from a reflectivity study of cesium-enriched sols, and is comparable to the density of ions in layer 2, Γ_2^+ , which points to the crystallization of layer 2. Alternatively, the surface may only be partially covered by the crystallites in layer 1 (~ 6 nm in diameter), so that the total surface charge density associated with the Na⁺ crystal would be lower than Γ_0^+ . Unfortunately, all layers scatter x rays coherently, so that separating the layers' contributions to the scattering intensity based on the present data is a complicated problem. In further experiments I plan to investigate the dependence of the in-plane structure of the compact layer on the size of the silica particles in the hydrosol, which could help in revealing precisely the positioning of the crystals in the compact layer from the alterations in the mosaicity of the surface.

Finally, ions adsorbed at the silica hydrosol's surface can be considered as a heavy, very dense analog of the two-dimensional system of electrons suspended above the surfaces of certain cryogenic dielectrics (liquid ³He and ⁴He, and liquid and solid hydrogen) by the image force and an external electrostatic field.^{25,26} The energy W of an ion in the two-dimensional lattice, defined by Coulomb interaction with the ions within the correlation length ($\sim 10^2$) in the lattice, is roughly as high as $W \sim 30e^2/(4\pi\epsilon_0\epsilon a) \sim 200k_B T - 400k_B T$ (where e is elementary charge, ϵ_0 is the dielectric permittivity of the vacuum, and $\epsilon \sim 10$), which is comparable with the hydration energy of Na⁺ in water ($\sim 160k_B T$). Others previously observed a solid phase of "classical" two-dimensional electrons (a Wigner crystal) at the surface of liquid helium when the ratio of potential to kinetic energy per electron becomes more than ~ 140 , i.e., comparable to $W/k_B T$.^{27,28} In those experiments, the temperature was much lower (~ 0.5 K) than in mine because the experimentally accessible range of surface densities of electron gases, for example, at the surface of liquid helium, is $\sim 10^4$ times smaller than the density of sodium ions at the sol's surface.

Use of the National Synchrotron Light Source, Brookhaven National Laboratory, was supported by the U.S. Department of Energy, Office of Science, Office of Basic Energy Sciences, under Contract No. DE-AC02-98CH10886.

X19C is partially supported through funding from the Chem-MatCARS National Synchrotron Resource, the University of Chicago, the University of Illinois at Chicago, and Stony Brook University. The author thanks Mark L. Schlossman, Vladimir I. Marchenko, Igor A. Zaliznyak, Alexander G. Abanov, and Anna I. Lygina for valuable discussions. The author also thanks Avril Woodhead for her comments on the paper.

- ¹M. A. Vorotyntsev and S. N. Ivanov, *Sov. Phys. JETP* **88**, 1729 (1985).
- ²I. Rouzina and V. A. Bloomfield, *J. Phys. Chem.* **100**, 9977 (1996).
- ³N. Gronbech-Jensen, R. J. Mashl, R. F. Bruinsma, and W. M. Gelbart, *Phys. Rev. Lett.* **78**, 2477 (1997).
- ⁴B. I. Shklovskii, *Phys. Rev. Lett.* **82**, 3268 (1999).
- ⁵J. J. Arenzon, J. F. Stilck, and Y. Levin, *Eur. Phys. J. B* **12**, 79 (1999).
- ⁶B. I. Shklovskii, *Phys. Rev. E* **60**, 5208 (1999).
- ⁷Y. Burak, D. Andelman, and H. Orland, *Phys. Rev. E* **70**, 016102 (2004).
- ⁸J. M. Bloch, W. B. Yun, X. Yang, M. Ramanathan, P. A. Montano, and C. Capasso, *Phys. Rev. Lett.* **61**, 2941 (1988).
- ⁹K. Kjaer, J. Als-Nielsen, C. Helm, P. Tippman-Krayer, and H. Möhwald, *J. Phys. Chem.* **93**, 3200 (1989).
- ¹⁰M. J. Bedzyk, G. M. Bommarito, M. Caffrey, and T. L. Penner, *Science* **248**, 52 (1990).
- ¹¹G. Luo, S. Malkova, J. Yoon, D. G. Schultz, B. Lin, M. Meron, I. Benjamin, P. Vanysek, and M. L. Schlossman, *Science* **311**, 216 (2006).
- ¹²D. Vaknin, P. Krüger, and M. Lösche, *Phys. Rev. Lett.* **90**, 178102 (2003); W. Bu, D. Vaknin, and A. Travesset, *Phys. Rev. E* **72**, 060501(R) (2005).
- ¹³C. Park, P. A. Fenter, K. L. Nagy, and N. C. Sturchio, *Phys. Rev. Lett.* **97**, 016101 (2006).
- ¹⁴A. M. Tikhonov, *J. Phys. Chem.* **111**, 930 (2007).
- ¹⁵A. M. Tikhonov, *J. Chem. Phys.* **124**, 164704 (2006).
- ¹⁶A. M. Tikhonov, *J. Phys. Chem. B* **110**, 2746 (2006).
- ¹⁷I. K. Robinson, *Phys. Rev. B* **33**, 3830 (1986).
- ¹⁸R. Feidenhansl, *Surf. Sci. Rep.* **10**, 105 (1989).
- ¹⁹V. M. Kaganer, H. Möhwald, and P. Dutta, *Rev. Mod. Phys.* **71**, 779 (1999).
- ²⁰M. L. Schlossman, D. Synal, Y. Guan, M. Meron, G. Shea-McCarthy, Z. Huang, A. Acero, S. M. Williams, S. A. Rice, and P. J. Viccaro, *Rev. Sci. Instrum.* **68**, 4372 (1997).
- ²¹The homogeneous monodispersed aqueous solution of 22 nm silica particles with bulk concentration, $c_b \approx 6 \times 10^{22} \text{ m}^{-3}$ had a specific gravity ρ of $1.257 \pm 0.004 \text{ g/cm}^3$ (40% of SiO_2 and 0.3% of Na by weight) and its specific surface area was $\sim 10^5 \text{ m}^2/\text{kg}$. The molar concentration of free hydroxyl ions in the bulk of the hydrosol is very small $c^- \sim 10^{-5} \text{ mol/L}$ ($\text{pH} \approx 9$) compared with the bulk concentration of sodium ions $c_{\text{Na}}^+ = f_{\text{Na}} \rho / M_{\text{Na}} \approx 0.05 \text{ mol/L}$ ($M_{\text{Na}} \approx 23 \text{ g/mol}$ is the atomic weight of Na, and f_{Na} is the weight fraction of sodium in the suspension) due to deprotonation of the silanol groups at the surface of silica particles by OH^- ions. Since $c^- \ll c^+$, the charge per particle in the sol $Z \approx e(c_{\text{Na}}^+ / c_b) \sim 500e$.
- ²²J. M. Sorenson, G. Hura, R. M. Glaeser, and T. Head-Gordon, *J. Chem. Phys.* **113**, 9149 (2000).
- ²³B. K. Vainshtein, *Modern Crystallography I: Symmetry of Crystals, Methods of Structural Crystallography* (Springer-Verlag, Berlin, 1981).
- ²⁴A. Guinier, *X-ray Diffraction Crystals, Imperfect Crystals and Amorphous Bodies* (Dover, New York, 1994).
- ²⁵The de Broglie wavelength for the thermal motion of alkali ions at room temperature is $\lambda_B = 2\pi\hbar/p \sim 0.1 - 1 \text{ \AA}$, where \hbar is Plank's constant and p is the momentum of thermal motions of the alkali ions $p \sim \sqrt{3k_B T m}$ (k_B is Boltzmann's constant and m is the mass of the alkali atoms). Since $l_{1,2} \gg \lambda_B$, Na^+ ions can be considered as "classical" particles.
- ²⁶V. S. Edel'man, *Sov. Phys. Usp.* **23**, 227 (1980).
- ²⁷R. S. Crandall and R. Williams, *Phys. Lett.* **34A**, 404 (1971).
- ²⁸C. C. Grimes and G. Adams, *Phys. Rev. Lett.* **42**, 795 (1979).